Chloride Channels Activated by Osmotic Stress in T Lymphocytes

RICHARD S. LEWIS, PAUL E. ROSS, and MICHAEL D. CAHALAN

From the Department of Physiology and Biophysics, University of California, Irvine, California 92717; and the Department of Molecular and Cellular Physiology, Stanford University School of Medicine, Stanford, California 94305

ABSTRACT We have used whole-cell and perforated-patch recording techniques to characterize volume-sensitive Cl^- channels in T and B lymphocytes. Positive transmembrane osmotic pressure (intracellular osmolality > extracellular osmolality) triggers the slow induction of a Cl^- conductance. Membrane stretch caused by cellular swelling may underlie the activation mechanism, as moderate suction applied to the pipette interior can reversibly oppose the induction of Cl^- current by an osmotic stimulus. Intracellular ATP is required for sustaining the Cl^- current. With ATP-free internal solutions, the inducibility of Cl^- current declines within minutes of whole-cell recording, while in whole-cell recordings with ATP or in perforated-patch experiments, the current can be activated for at least 30 min. The channels are anion selective with a permeability sequence of $I^- > SCN^- > NO_3^-$, $Br^- > Cl^- > MeSO_3^-$ > acetate, propionate > ascorbate > aspartate and gluconate. G_{Cl} does not show voltage- and time-dependent gating behavior at potentials between −100 and +100 mV, but exhibits moderate outward rectification in symmetrical Cl^- solutions. Fluctuation analysis indicates a unitary chord conductance of ~2 pS at −80 mV in the presence of symmetrical 160 mM Cl^-. The relationship of mean current to current variance during the osmotic activation of Cl^- current implies that each cell contains on the order of 10^4 activatable Cl^- channels, making it the most abundant ion channel in lymphocytes yet described. The current is blocked in a voltage-dependent manner by DIDS and SITS (K_i = 17 and 89 μM, respectively, at +40 mV), the degree of blockade increasing with membrane depolarization. The biophysical and pharmacological properties of this Cl^- channel are consistent with a role in triggering volume regulation in lymphocytes exposed to hyposmotic conditions.

INTRODUCTION

Volume regulation is a widespread process that enables cells to maintain their normal volume in the face of changes in extracellular osmolarity. This ability to control cell volume may have evolved as an essential mechanism enabling primitive cells to survive and function in environments of varying osmolarity. A variety of solute and water transport mechanisms have been proposed to account for volume regulation in

Address reprint requests to Dr. Richard S. Lewis at his present address: Department of Molecular and Cellular Physiology, Stanford University School of Medicine, Stanford, CA 94305.

J. GEN. PHYSIOL. © The Rockefeller University Press · 0022-1295/93/06/0801/26 $2.00
Volume 101 June 1993 801–826

different cells; the common feature of these models is the transport of ions across the cell membrane followed by osmotically obliged water (for review see Hoffmann and Simonsen, 1989). Among mammals with efficient renal mechanisms for controlling the tonicity of extracellular fluid, large changes in osmolarity are only seen within the kidney and the small intestine. In such organisms, the ability of cells to volume regulate in response to osmotic challenge may therefore reflect an ongoing homeostatic control mechanism that fine-tunes cellular water flux, for example, to ensure coordinated transport of water across epithelia. Volume regulatory mechanisms may also be important for growth during the cell cycle.

Grinstein and his colleagues have investigated two distinct mechanisms of volume regulation in lymphocytes exposed to hyperosmotic or hyposmotic solutions (reviewed by Deutsch and Lee, 1988; Grinstein and Dixon, 1989). Hyperosmotic solutions induce water efflux, cell shrinkage, phosphorylation of a variety of cellular substrates, and activation of a sodium-hydrogen exchange mechanism which results in a subsequent regulatory volume increase (RVI). Upon exposure to hyposmotic solutions, lymphocytes initially swell as water enters but shrink over a period of minutes to nearly the normal volume. Based on measurements of cell volume, membrane potential, and ion fluxes, it has been shown that regulatory volume decrease (RVD) involves separate conductive pathways for Cl^- and K^+ (Grinstein, Clarke, Dupre, and Rothstein, 1982; Sarkadi, Mack, and Rothstein, 1984*a*, *b*). The membrane conductance to both Cl^- and K^+ ions is increased by cell swelling, resulting in efflux of both ions and osmotically obliged water efflux.

Previous patch-clamp studies have revealed a diversity of ion channels which appears to underlie a variety of functions in T lymphocytes, including mitogenic activation and volume regulation (for review see Lewis and Cahalan, 1990). A voltage-gated potassium channel, termed type *n*, appears to be the predominant channel in normal human T cells under resting conditions. Pharmacological blockade of K^+ channels has indicated a requirement for type *n* K^+ channels in the activation of T lymphocytes by mitogens. Two lines of experimental evidence suggest that type *n* channels may also underlie K^+ efflux during RVD (for review see Deutsch and Lee, 1988). First, a variety of K^+ channel blockers inhibit RVD. Second, studies of T cell lines and B lymphocytes have shown that the ability to volume regulate parallels the level of expression of type *n* channels. A second class of K^+ channels in T cells is activated by a rise in cytosolic free calcium concentration, $[Ca^{2+}]_i$. These calcium-dependent K^+ (K_{Ca}) channels may play a role in mitogen-induced calcium signaling (Grissmer, Lewis, and Cahalan, 1992), and while it was originally suggested that they may also be involved in RVD, recent evidence suggests that they are not essential in this regard (Rink, Sanchez, Grinstein, and Rothstein, 1983; Grinstein and Dixon, 1989; Grinstein and Smith, 1990).

In this article, we describe the properties of low-conductance ("mini") Cl^- channels revealed during whole-cell recording from T lymphocytes, as first reported by Cahalan and Lewis (1988). The properties of these channels, in particular their activation by osmotically induced cell swelling, their ion selectivity, and their pharmacological sensitivities, suggest an involvement in the Cl^- efflux pathway triggered during RVD. A careful comparison of biophysical properties, including voltage dependence, rectification, ion selectivity, and pharmacological sensitivities,

may facilitate comparisons to Cl^- channels found in other cells, such as the low-conductance Cl^- channels in mast cells (Matthews, Neher, and Penner, 1989) and chromaffin cells (Doroshenko and Neher, 1992), as well as swelling-activated Cl^- channels in epithelial cells (McCann, Li, and Welsh, 1989; Worrell, Butt, Cliff, and Frizzell, 1989; Solc and Wine, 1991; Chan, Goldstein, and Nelson, 1992). Similarities in properties of Cl^- channels in several cell types suggest that osmotically activated Cl^- channels in lymphocytes may be members of a widely distributed class of channels whose mode of activation is tailored to cell-specific functions.

A portion of this work has been published in preliminary form (Cahalan and Lewis, 1988).

METHODS

Cell Isolation

Thymocytes were isolated from the thymuses of 4–8-wk-old BALB/c, C57BL/6, or NIH-Swiss mice following standard procedures (Lewis and Cahalan, 1988). In some experiments, thymocyte subsets were stained with fluorescein-labeled anti-CD8 antibody and phycoerythrin-labeled anti-CD4 and identified under epifluorescence illumination as described (Lewis and Cahalan, 1988). Splenocytes were flushed from the spleens of adult mice by splenic puncture and perfusion and were subsequently washed and resuspended in RPMI 1640 medium containing 25 mM HEPES and 2 mM glutamine supplemented with 10% fetal bovine serum (FBS). In some experiments, T cells were isolated by passing the splenocytes through a nylon wool column followed by elution with warm RPMI medium containing 20% FBS. Cells were generally used within 2–12 h of isolation; in some experiments, cells were stored in medium at 4°C until use the next day.

The human helper T leukemia cell line, Jurkat E6-1, was obtained from American Type Culture Collection (ATCC; Rockville, MD) and maintained in RPMI + 10% FBS following standard procedures. Human T cells were isolated from the peripheral blood of healthy human volunteers by centrifugation in Ficoll-Hypaque (Pharmacia Fine Chemicals, Piscataway, NJ) followed by passage through a nylon wool column as described above, and were kept in medium until use the same day. The Epstein-Barr virus (EBV)–transformed human B lymphoblast line GM03299A was obtained from the NIGMS Human Genetic Mutant Cell Repository and maintained in RPMI + 10% FBS.

Recording Techniques

Before recording in most experiments, cells were allowed to settle on coverslip chambers that had been pretreated with 0.2–0.5 mg/ml poly-D-lysine (Sigma Chemical Co., St. Louis, MO) for 15 min at room temperature. In many cases, Jurkat cells adhered adequately to untreated clean glass substrate; however, the use of polylysine did not appear to change the inducibility or properties of the Cl^- conductance described here. Standard whole-cell and perforated-patch recording techniques were applied (Hamill, Marty, Neher, Sakmann, and Sigworth, 1981; Horn and Marty, 1988; Lewis and Cahalan, 1989). Recording pipettes were pulled from soft glass capillaries (Accu-fill 90 Micropets; Becton, Dickinson & Co., Parsippany, NJ), coated with Sylgard (Dow Corning Corp., Midland, MI) near their tips, and fire polished to give resistances of 2–8 MΩ when filled with internal solution and immersed in Ringer's solution. All membrane voltages were corrected for the junction potential arising between the recording pipette and the bath solution in which the pipette current was nulled before seal formation. In addition, we applied corrections for junction potentials between the bath solution and the ground reference

(a Ringer-containing agar bridge) resulting from the exchange of extracellular anions. Relative junction potentials of anion-substituted Ringer's solutions had the following values in millivolts: I^-, 0; SCN^-, 0; Br^-, 0; NO_3^-, −1; $MeSO_3^-$, −5; acetate, −6; propionate, −8; aspartate, −10; gluconate, −10; ascorbate, −11. Cell membrane and pipette capacitance were canceled using electronic feedback via the patch-clamp amplifier (AxoPatch 1-D, Axon Instruments, Inc., Foster City, CA; or List L/M-EPC-7, Medical Systems Corp., Greenvale, NY). A PDP-11/73 computer and interface running programs written in BASIC-23 were used to generate voltage commands and to digitize and analyze the patch-clamp current output (Indec Systems, Inc., Sunnyvale, CA). Unless otherwise noted, all data were corrected for leak current. Leak current was collected in response to voltage ramps presented immediately after establishing whole-cell configuration ("break-in"), before the induction of Cl^- current by osmotic stimuli, and was generally much smaller than the induced Cl^- conductance (e.g., see Fig. 1 *A*).

Series resistance compensation was not used in these experiments. The resulting errors in membrane potential, current magnitude, and frequency response were in general judged to be insignificant for the conclusions of this study. Maximal chloride current amplitudes were usually

TABLE I

Internal Solutions

Solution name	Aspartic or glutamic acid	$MgCl_2$	$CaCl_2$	EGTA	Na_2ATP or NaGlu	HEPES	Sucrose	Osmolarity
								mosM
K Asp	160	2	0.1	1.1	—	10	—	310
K Asp + ATP	160	2	0.1	1.1	4	10	—	320
K Asp + ATP (hyperosmotic)	160	2	0.1	1.1	4	10	114	440
K Asp + ATP (isosmotic)	140	2	—	11	4	10	—	315
Cs Glu	160	2	0.1	1.1	8	10	—	315
Cs Glu + ATP	160	2	0.1	1.1	4	10	—	315
Cs Glu (hyperosmotic)	160	2	0.1	1.1	8	10	100	420
Cs Glu + ATP (hyperosmotic)	160	2	0.1	1.1	4	10	100	420

pH of all solutions was adjusted to 7.2 with KOH or CsOH. In some experiments, Cs^+ was substituted for K^+ or KCl was substituted for aspartic acid.

< 500 pA and only occasionally as large as 1 nA; a 10-MΩ series resistance (R_s) would therefore cause a maximal voltage error of 5–10 mV. Slope Cl^- conductance was measured at potentials within a 10–20-mV range centered on the Cl^- reversal potential, E_{Cl} (Cahalan and Lewis, 1988), and because the current approaches zero near E_{Cl}, the error due to uncompensated R_s is negligible. The series resistance (10 MΩ maximum) in series with membrane capacitance (8 pF maximum) is estimated to cause first-order rolloff at frequencies $> 1/(2\pi R_s C_m)$, or at least 1,990 Hz. This frequency is sufficiently far above the cutoff frequency for Cl^- channel gating (~300 Hz) so as not to significantly affect our estimates of variance and spectral density. All experiments were conducted at room temperature (22–25°C). Grouped data are given as mean ± SD.

Solutions

The composition of internal solutions for whole-cell recording is given in Table I. Solution osmolarity was measured with a vapor pressure osmometer (Wescor Inc., Logan, UT). For perforated-patch experiments, nystatin (Sigma Chemical Co.) stock solution in dimethylsulfoxide was suspended by vortexing (Vortex-Genie 2; Scientific Industries, Bohemia, NY) at a final

concentration of 100 μg/ml in a pipette solution containing (mM): 55 KCl, 70 K_2SO_4, 7 $MgCl_2$, 5 D-glucose, and 10 HEPES, titrated to pH 7.2 with KOH. Bath solutions were exchanged by perfusing the chamber (volume of ~250 μl) with 2–5 ml of test solution. Exchange was complete in <30 s. In ion-exchange experiments, exposure to the test ion was preceded and followed by exposure to normal Ringer to verify that pipette potential had not drifted during the measurement. Cells were bathed in Ringer's solution consisting of (mM): 160 NaCl, 4.5 KCl, 2 $CaCl_2$, 1 $MgCl_2$, and 5 HEPES, titrated to pH 7.4 with NaOH (310 mosM). Hyposmotic Ringer's was made by dilution with distilled H_2O. Anion-substituted Ringer's solutions, with the exception of SCN^-, were prepared using the hydroxide salts of Na^+, K^+, Mg^{2+}, and Ca^{2+} and the appropriate acid. SCN^- Ringer's consisted of (mM): 160 NaSCN, 4.5 KCl, 2 $CaCl_2$, 1 $MgCl_2$, and 5 HEPES, titrated to pH 7.4 with NaOH. Acetic, gluconic, hydrobromic, hydroiodic, methanesulfonic, and nitric acids were obtained from Aldrich Chemical Co. (Milwaukee, WI); ascorbic acid, aspartic acid, propionic acid, sodium thiocyanate, 4,4′-diisothiocyanatostilbene-2,2′-disulfonic acid (DIDS), 4-acetamido-4′-isothiocyanatostilbene-2,2′-disulfonic acid (SITS), 1,9-dideoxyforskolin, and verapamil were obtained from Sigma Chemical Co.

Current Fluctuation Analysis

Whole-cell current was recorded during the induction of g_{Cl} at a bandwidth of 6 kHz (8-pole Bessel filter; Frequency Devices Inc., Haverhill, MA) onto VCR tape (PCM; Unitrade, St. Louis, MO). For mean-variance analysis, data were replayed off-line through a 2-kHz Bessel filter and digitized at a rate of 10 kHz. The mean and variance were computed for 100-ms sweeps collected at 1-s intervals. Data for spectral analysis were played back through a 5-Hz high-pass (Krohn-Hite Corp., Avon, MA) and a 6-kHz low-pass Butterworth filter (Frequency Devices Inc.) in series, and digitized at a rate of 12.5 kHz. After subtracting the average current level from each of 64 sweeps (512 points per sweep), power spectra were computed and averaged. The spectrum of the background whole-cell–current noise collected before induction of the chloride conductance was subtracted from the averaged test spectrum.

RESULTS

Results are presented below in two parts: first, a description of the activation of Cl^- channels in T cells, and second, an analysis of their biophysical and pharmacological properties.

"Spontaneous" Induction of Cl^- Current

In the majority of recordings conducted with K^+ aspartate internal solutions containing ATP (see Table I), a Cl^- conductance developed spontaneously within several minutes of establishing the whole-cell configuration. The induction of Cl^- current is most easily observed using voltage-ramp stimuli; the Cl^- current is displayed accurately in ramps because the conductance is neither time nor voltage dependent (see below). Fig. 1 *A* shows a series of currents evoked by voltage ramps from −100 to +20 mV in a splenic T cell. In this cell, an outwardly rectifying current began to appear after ~50 s of whole-cell recording. The current is easily distinguished from a possible increase in nonselective leak by its reversal potential (V_{rev}) of −46 mV (Fig. 1 *C*). In some cells, a component of current developed that reversed near 0 mV, presumably reflecting an increase in leak or seal conductance, but these cells were excluded from the analysis presented here. In all experiments that follow, V_{rev} for the Cl^- current was relatively constant over time (Fig. 1 *C*). The conduc-

tance's selectivity for Cl^- is indicated by its reversal potential and the results of ion-substitution experiments (described in detail below). As illustrated in Fig. 1 *A*, the Cl^- current could be observed in relative isolation in splenic T lymphocytes since these cells express only 5–10 voltage-gated K^+ channels per cell (DeCoursey,

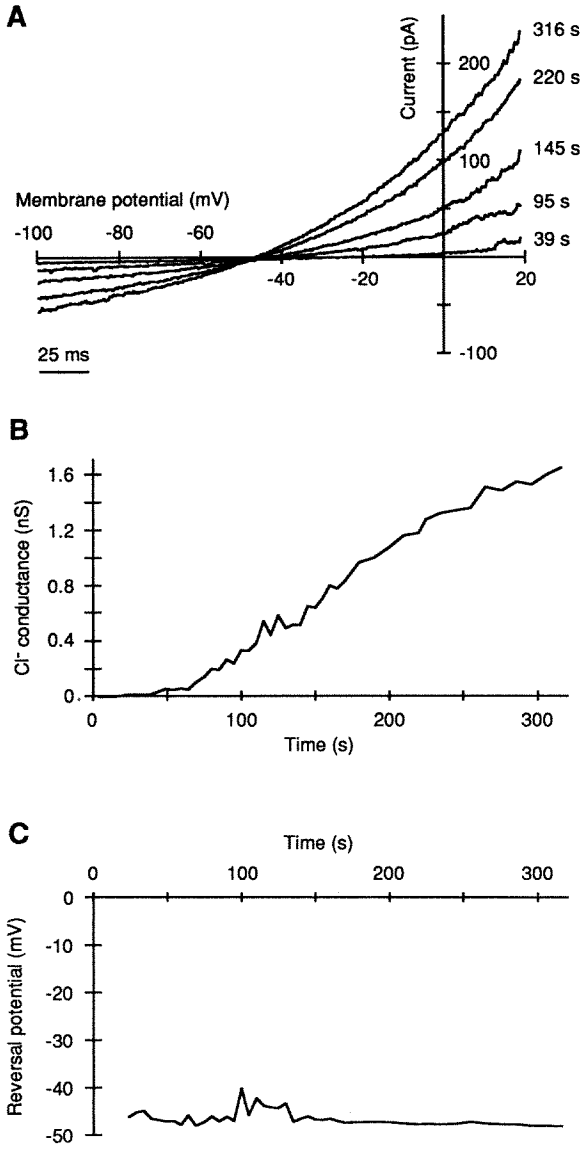

FIGURE 1. Spontaneous induction of Cl^- conductance in a splenic T lymphocyte. (*A*) A series of whole-cell currents elicited by 256-ms voltage ramps from −100 to +20 mV. Time elapsed since establishing the whole-cell configuration (break-in) is indicated in seconds next to each sweep. In this cell, a small amount of voltage-dependent K^+ current is also present at positive potentials. Leak current has not been subtracted from the records shown. (*B*) Slope Cl^- conductance (g_{Cl}) plotted against time after break-in. g_{Cl} at 5-s intervals was determined from a linear least-squares fit to the current–voltage relation at potentials between −38 and −55 mV (see Methods; Cahalan and Lewis, 1988). (*C*) Reversal potential (V_{rev}) plotted against time in the same experiment. Cell 153; K Asp + ATP internal solution (see Table I).

Chandy, Gupta, and Cahalan, 1987; Lewis and Cahalan, 1988); in human T cells and Jurkat T cells, which contain 100–300 K^+ channels per cell, internal Cs^+ or extracellular charybdotoxin (Sands, Lewis, and Cahalan, 1989) was used to block the K^+ conductance and thereby isolate the Cl^- current for study.

Cl^- Current Induction by the Transmembrane Osmotic Gradient

Several lines of evidence support the notion that the transmembrane osmotic gradient regulates activation of Cl^- conductance. First, exposure of cells to hyperosmotic external solutions such as Ringer + 100 mM sucrose quickly reverses the spontaneous development of Cl^- current described above (Cahalan and Lewis, 1988).

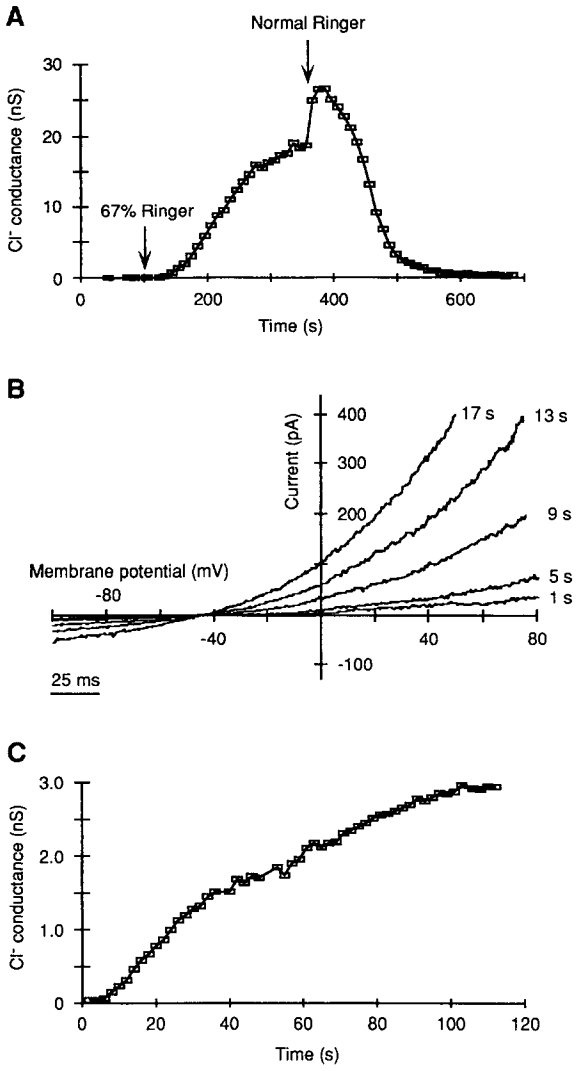

FIGURE 2. Cl^- conductance is controlled by the transmembrane osmotic gradient. (*A*) Reversible activation of g_{Cl} in a Jurkat T cell by hyposmotic extracellular solution (67% Ringer). Slope g_{Cl} is plotted against time after break-in. Spontaneous induction of g_{Cl} was prevented by the use of osmotically balanced internal solution. Cell 904; KCl + ATP, isosmotic. (*B*) Hyperosmotic internal solution elicits rapid activation of Cl^- conductance in a $CD4^+$ mouse splenic T cell. Induction of g_{Cl} is much more rapid than the spontaneous induction pictured in Fig. 1. Cell 364; K asp + ATP, hyperosmotic. (*C*) Hyperosmotic internal solution accelerates the time course of Cl^- current induction, which begins within several seconds of establishing whole-cell configuration. Data are from the experiment in *B*.

Moreover, when the osmolarity of the internal solution was adjusted to match that of the bath solution, the Cl^- conductance did not appear during whole-cell recording. Finally, exposure to hyposmotic extracellular solution evokes prompt and robust Cl^- current activation. In the experiment shown in Fig. 2 *A*, bath perfusion with hyposmotic Ringer (diluted to 67% of its normal osmolarity) elicited a delayed

increase of Cl^- conductance which rose to a steady-state level after 200–300 s. After reintroduction of normal Ringer, g_{Cl} increased transiently, presumably due to the increased external Cl^- concentration, and then declined as Cl^- channels were deactivated. Additional experiments suggest that the conductance is regulated by the transmembrane osmotic gradient rather than the absolute osmolarity of the extracellular environment. As illustrated in Fig. 2, *B* and *C*, g_{Cl} activates within seconds of establishing the whole-cell configuration with a hyperosmotic internal solution (K^+ aspartate + 114 mM sucrose). Under these conditions, the induction latency is significantly shorter and the maximal amplitude of g_{Cl} greater than that observed with a more moderate osmotic imbalance (cf. Fig. 1). Thus, conditions that create a transmembrane osmotic gradient control Cl^- current activation in T cells; when expressed as extracellular relative to intracellular, hyposmotic conditions activate g_{Cl} while hyperosmotic conditions deactivate it.

Osmotic Activation Occurs through Membrane Stretch

One possible mechanism for Cl^- conductance activation is hypotonic cell swelling. In fact, during activation of g_{Cl} in T cells by hyposmotic solutions, we often observed an increase in cell diameter indicative of swelling, suggesting that membrane stretch may be necessary for g_{Cl} activation. To test this idea, suction was applied to the recording pipette during the induction of g_{Cl} by hyposmotic Ringer. As shown in Fig. 3 *A*, negative pressure applied to the pipette (−20 cm H_2O; −2 kPa) deactivates the conductance. Relieving the pipette pressure allows activation to proceed, while application of positive pressure (10 cm H_2O; 1 kPa) appears to accelerate the rate of activation. Negative pipette pressure also terminates the rise in g_{Cl} induced by hyperosmotic pipette solution (Fig. 3 *B*). Positive pressure applied to cells under isosmotic conditions was also sufficient to induce Cl^- current (not shown). Taken together, these results are consistent with a mechanism of activation involving membrane stretch, although they do not necessarily imply direct sensing of mechanical forces by the channel's gating mechanism (see Discussion).

Dependence of Cl^- Conductance on Intracellular ATP

In the experiments described above, osmotic activation of Cl^- current was found to require ATP in the pipette solution. In recordings from Jurkat T cells with pipettes containing ATP, the Cl^- conductance could be induced repeatedly by hypotonic challenge over a period of > 10 min (Fig. 4 *A*). In the absence of added internal ATP, the inducibility of g_{Cl} fell to near zero over a similar time period (Fig. 4 *B*). The time course of this washout effect varied somewhat from cell to cell, and tended to be accelerated in smaller cells. For example, in murine T cells, which are roughly half the diameter of Jurkat cells, we were unable to detect osmotically activated Cl^- current in the absence of added ATP even within 1 min of break-in, while Jurkat cells often displayed a modest Cl^- current at these times (Fig. 4 *B*). These results suggest that the inducibility of Cl^- conductance declines as ATP is removed from the cell cytoplasm at a rate determined by the efficacy of internal dialysis through the recording pipette. This conclusion is also consistent with observations that ATP is required in the recording pipette to sustain a constant elevated level of g_{Cl}; without

ATP, continued hyposmotic exposure elicits only a transient increase of g_{Cl} (Ross, Garber, and Cahalan, 1992).

While they support the idea that ATP is required for Cl^- channel activity, the above results do not rule out the possibility that induction of Cl^- conductance also requires removal of an endogenous inhibitory factor. To test this possibility, we conducted perforated-patch recordings from Jurkat cells. With this technique, in which nystatin

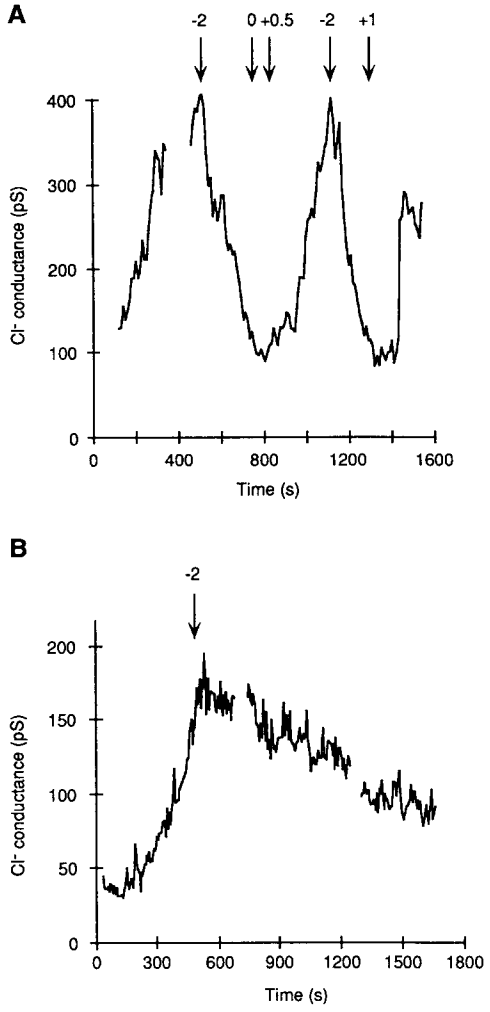

FIGURE 3. Osmotic activation of g_{Cl} is modulated by pipette hydrostatic pressure. (*A*) After activation by 67% Ringer, g_{Cl} is reduced by suction applied to the cell's interior through the recording pipette. Cell 501; Cs Glu + ATP, isosmotic. (*B*) Negative pipette pressure reverses the rise in g_{Cl} activated by hyperosmotic pipette solutions. Cell 198; Cs Glu + ATP, hyperosmotic. Jurkat cells were used in both experiments, and pipette pressure is indicated in units of kPa.

in the recording pipette is used to provide electrical access to the cell's interior (Horn and Marty, 1988), we could often record membrane currents over a period of >30 min while preventing the escape of low molecular weight solutes such as fura-2 (Lewis and Cahalan, 1989). In the perforated-patch configuration, g_{Cl} could be activated in Jurkat cells by osmotic stimuli for periods of >20 min (Fig. 4 *C*). These results indicate that removal of an endogenous regulatory factor is not necessary for Cl^-

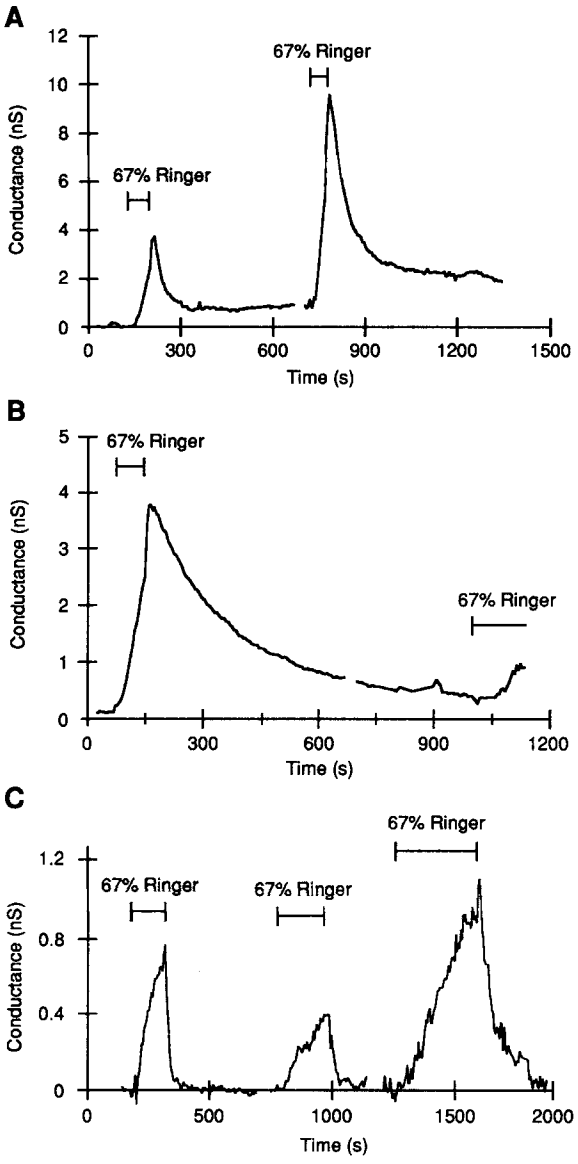

FIGURE 4. Activation of Cl^- channels requires intracellular ATP. (*A*) With ATP present in the recording pipette, g_{Cl} is inducible by osmotic challenge at least 10 min after the start of whole-cell recording. Cell 314; 90% Cs Glu + ATP, isosmotic, 10% dH_2O. (*B*) Without ATP in the recording pipette, induction of g_{Cl} by hypotonic shock is diminished after 16 min of whole-cell recording. This cell died at the end of the recording. Cell 321; 90% Cs Glu, isosmotic, 10% dH_2O. (*C*) In the perforated-patch mode, g_{Cl} remains inducible for long periods, even though an exogenous source of ATP is not present. Cell 884. All three recordings were obtained from Jurkat cells.

current activation. Furthermore, taken together with the results of Fig. 4, *A* and *B*, the perforated-patch data imply that endogenous ATP, which escapes the cell by dialysis during conventional whole-cell recording, is a critical cellular component necessary for Cl^- channel activation.

Ionic Selectivity

To measure the ionic selectivity of the Cl^- conductance, extracellular ions were substituted for Na^+ or Cl^- after induction of g_{Cl} by hyperosmotic internal solutions.

Two experiments indicate that the osmotically activated current of T cells is not significantly permeable to cations. First, after activation of g_{Cl} by 67% Ringer (114 mM Cl^-), perfusion with normal Ringer (170 mM Cl^-) shifted the reversal potential by -7.1 ± 1.0 mV ($n = 5$). For a perfectly anion-selective current, a shift of -10 mV would be expected; the observed shift indicates that the conductance is ~20-fold more permeant to anions than cations. Second, even though its reversal potential of -45 to -55 mV might suggest a permeability to K^+, total replacement of extracellular Na^+ by K^+ does not alter the current (Fig. 5*A*). In contrast, the effects of replacing extracellular Cl^- with a variety of anions reveal a substantial anion permeability. NO_3^-, Cl^-, Br^-, I^-, $MeSO_3^-$, SCN^-, ascorbate, acetate, aspartate, gluconate, and propionate were found to carry current through the channels. Relative permeabilities were estimated by reversal potentials according to a modified Goldman-Hodgkin-Katz equation:

$$V_{rev} = \frac{RT}{zF} \ln \frac{P_x[X^-]_o + P_{Cl}[Cl^-]_o + P_C[C^+]_i}{P_{asp}[asp^-]_i + P_{Cl}[Cl^-]_i + P_C[C^+]_o} \quad (1)$$

where R is the universal gas constant, T is the temperature, z is the valence (-1), F is Faraday's constant, and P_x, P_{Cl}, and P_C are the respective permeabilities of the test anion, Cl^-, and cations. Assuming constant intracellular anion concentrations and equimolar substitution of X^- for Cl^- ($[X^-]_o = [Cl^-]_o$), Eq. 1 reduces to

$$\frac{P_x}{P_{Cl}} = \frac{([Cl^-]_o + P_C/P_{Cl}[C^+]_i)e^{(zF/RT)(V_x - V_{Cl})} - P_C/P_{Cl}[C^+]_i}{[X^-]_o} \quad (2)$$

where V_x and V_{cl} are reversal potentials measured with extracellular X^- or Cl^-, respectively. Representative examples of ramp currents in the presence of extracellular Cl^-, $MeSO_3^-$, aspartate, and NO_3^- are shown in Fig. 5, *B* and *C*. Eq. 2 was used to calculate relative permeabilities for each anion and yielded the results shown in Table II. To check the assumptions made in Eq. 2, we also calculated P_{asp}/P_{Cl} using Eq. 1 and the reversal potential measured in normal Ringer. From the measured average V_{rev} of -47 ± 2 mV ($n = 12$) in the presence of internal 160 mM aspartate and 4 mM Cl^- and external 170 mM Cl^-, the relative permeability to aspartate (P_{asp}/P_{Cl}) is 0.11 ± 0.01. This result agrees well with the value of 0.11 ± 0.05 ($n = 12$) obtained from external aspartate substitution and Eq. 2. Measured reversal potentials were reproducible after exposure to foreign anions with the exception of acetate and propionate. Prolonged exposure to these anions induced membrane leakage in some cases, possibly due to intracellular acidification. The overall sequence of permeabilities is $I^- > SCN^- > NO_3^-$, $Br^- > Cl^- > MeSO_3^-$ > acetate, propionate > ascorbate > aspartate, gluconate.

The relative conductance for each of the anions, indicative of each anion's ability to carry current through the Cl^- channel, was estimated by the slope of the current–voltage curve at the reversal potential. Because at the reversal potential efflux of aspartate and Cl^- is equal to influx of the test anion, this method provides a relatively unbiased estimate of the relative conductance for each test anion. The conductance sequence was similar to the permeability sequence, with the exception that SCN^- was the most effective anion at carrying current through the channels; the complete

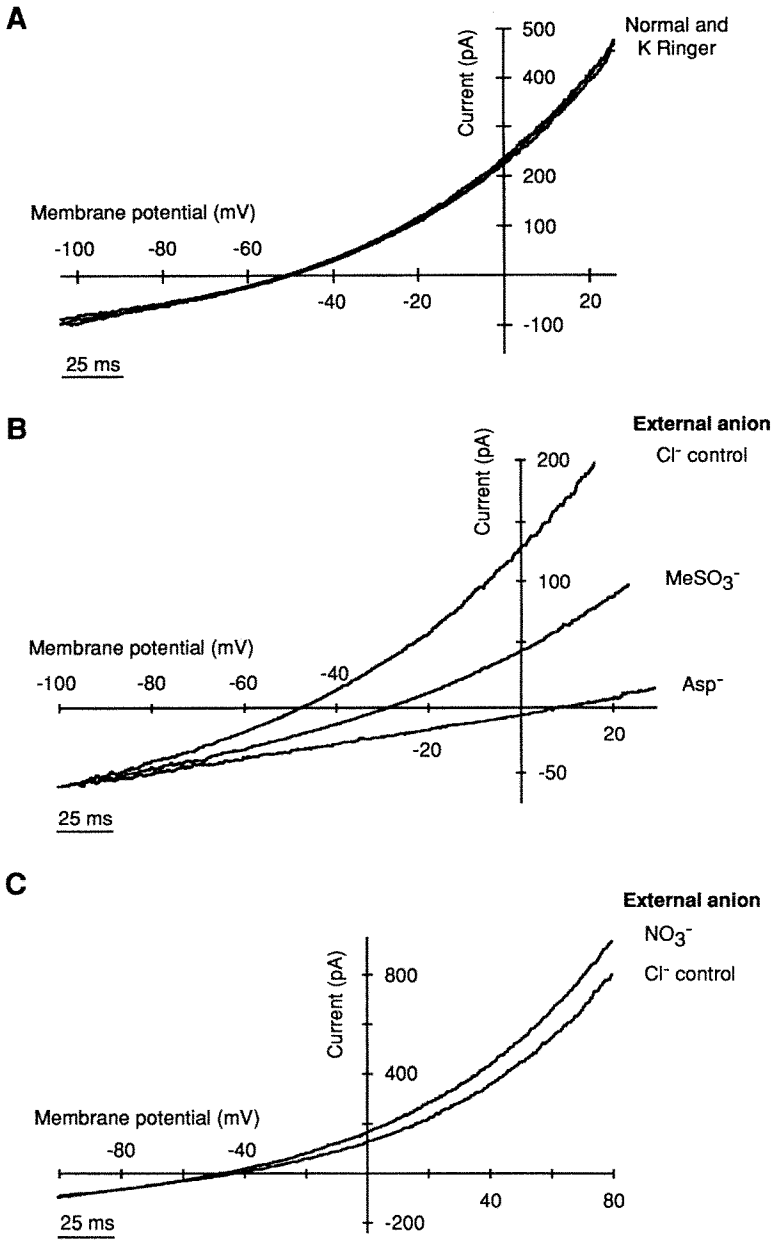

FIGURE 5. Ionic selectivity of the Cl^- conductance. (*A*) Ramp currents recorded before, during, and after substitution of K^+ for extracellular Na^+. Cell 69; K asp + ATP. (*B*) Ramp currents recorded before and after substitution of $MeSO_3^-$ or aspartate for extracellular Cl^-. Cell 120; K asp + ATP. (*C*) Ramp currents recorded before and after replacing extracellular Cl^- with NO_3^-. Cell 518; Cs asp + ATP + 30 mM sucrose. All three recordings are from murine splenic T cells.

conductance sequence is $SCN^- > I^-, NO_3^-, Br^- > Cl^- > MeSO_3^-$, acetate, propionate > ascorbate, aspartate, gluconate.

Lack of Voltage Dependence

The gating of osmotically activated Cl^- channels in T cells is not detectably voltage dependent. As illustrated in Fig. 6 *A*, outwardly rectifying Cl^- current is constant during voltage steps from −80 to +60 mV, without evidence of a time-dependent opening or closing of the channels. This lack of time dependence extends to potentials at least as positive as +100 mV (see Fig. 9). The amplitudes of Cl^- currents elicited by voltage steps agree closely with that of the ramp current recorded from the same cell (Fig. 6 *B*), suggesting that the outward rectification seen in ramp currents is due to permeation properties rather than to voltage- and time-dependent gating.

TABLE II

Relative Anion Permeability and Conductance of Cl^- Channels

Anion	$V_x - V_{Cl}$	P_x/P_{Cl}	G_x/G_{Cl}
	mV		
I^-	−7.2 ± 1.7 (4)	1.35 ± 0.10 (4)	1.12 ± 0.07 (3)
SCN^-	−5.1 ± 2.5 (7)	1.23 ± 0.12 (7)	1.28 ± 0.32 (7)
NO_3^-	−3.7 ± 0.3 (3)	1.17 ± 0.02 (3)	1.07 ± 0.07 (3)
Br^-	−3.7 ± 1.0 (3)	1.17 ± 0.05 (3)	1.13 ± 0.14 (3)
Cl^-	0	1.0	1.0
$MeSO_3^-$	19.6 ± 2.4 (4)	0.43 ± 0.05 (4)	0.69 ± 0.03 (6)
Acetate	26.3 ± 4.0 (5)	0.32 ± 0.06 (5)	0.64 ± 0.04 (5)
Propionate	30.0 ± 5.3 (3)	0.27 ± 0.07 (3)	0.69 ± 0.03 (3)
Ascorbate	37.0 ± 2.5 (4)	0.19 ± 0.03 (4)	0.48 ± 0.04 (4)
Aspartate	48.1 ± 8.3 (12)	0.11 ± 0.05 (12)	0.42 ± 0.07 (16)
Gluconate	50.2 ± 9.0 (13)	0.10 ± 0.06 (13)	0.42 ± 0.10 (13)

For each test anion, reversal potential (V_x) and slope conductance (G_x) at the reversal potential were used to calculate P_x/P_{Cl} and G_x/G_{Cl} (described in Results). Relative permeabilities were calculated assuming an extracellular concentration of 170 mM for each anion and a relative cation permeability (P_C/P_{Cl}) of 0.049. The number of measurements is indicated in parentheses.

What causes the outward rectification of the Cl^- current? In experiments in which Cl^- is the external anion and aspartate is the predominant internal anion (e.g., Fig. 6, *A* and *B*), outward rectification of the current–voltage relation is expected due to the low relative permeability of the channels to aspartate. However, outward rectification persists in symmetric internal and external chloride (Fig. 6 *C*). In principle, such nonlinearity could result from voltage-dependent channel block or from the location of permeation barriers within the channel pore. For example, both ATP and HEPES are anions at physiological pH, and intracellular HEPES and other morpholino-based anionic pH buffers have been reported to block inward current through Cl^- channels in *Drosophila* neurons (Yamamoto and Suzuki, 1987). However, in the presence of approximately symmetrical aspartate as the primary current carrier, the current–voltage relation appears to be linear even though HEPES and ATP are present (Fig. 5 *B*), arguing against voltage-dependent block by these compounds. An alternative explanation for these results is that the physical barriers

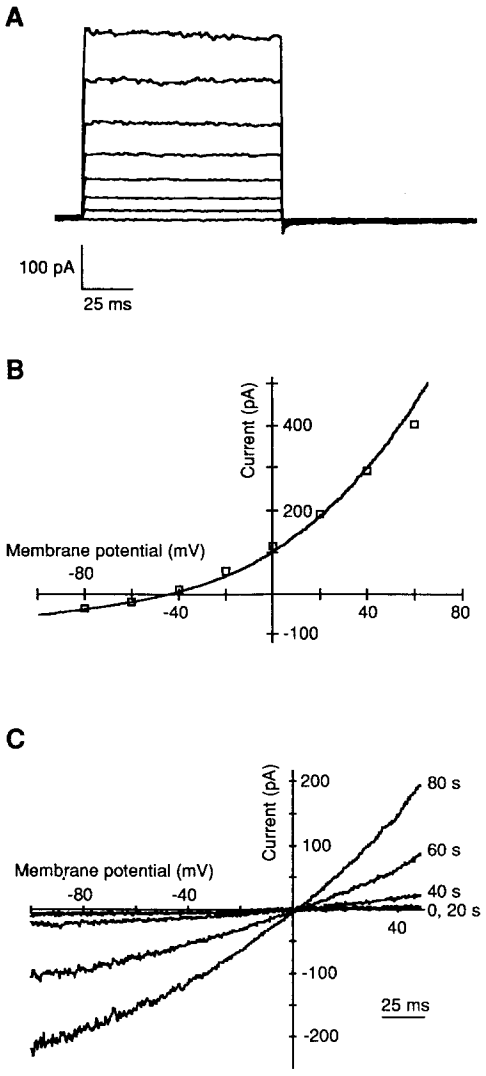

FIGURE 6. Gating of Cl^- channels is not voltage dependent. (*A*) Cl^- currents evoked in a $CD4^+$ splenic T cell by a series of 100-ms voltage steps from −80 to +60 mV. Data were not corrected for leakage or capacitative currents. Cell 399; K Asp + ATP. (*B*) Peak current values from *A* (symbols) plotted with the ramp current recorded from the same cell. (*C*) Outward current rectification in the presence of symmetrical intracellular and extracellular [Cl^-]. Ramp currents were recorded from a splenic T cell during induction of g_{Cl} at the times indicated to the right of each sweep. Cell 295; KCl + ATP.

controlling Cl^- permeation give rise to the outwardly rectifying characteristic in symmetrical Cl^-, and that their location is different from those that determine the permeability to aspartate.

Estimating the Unitary Conductance

Attempts to measure directly the currents through single Cl^- channels in cell-attached membrane patches were unsuccessful, due in part to the channel's small unitary conductance and its high surface density (see below). Instead, we estimated the conductance of the Cl^- channel by analyzing Cl^- current fluctuations at various times during its induction, based on the principles underlying mean-variance analysis of nonstationary currents (Sigworth, 1980). For a collection of identical, independent

channels with two conductance states (closed and open) obeying binomial statistics, the mean current, I, and variance around the mean current, σ_I^2, are related by the expression

$$\sigma_I^2 = iI - I^2/N \tag{3}$$

where i is the single-channel current amplitude and N is the number of activatable channels in the plasma membrane. The Cl^- current increases relatively slowly in response to hypotonic challenge, growing at a maximum rate of 15 pA/s in the experiment of Fig. 7, *A–C*, or 5 pA/s in the experiment of Fig. 7 *D*. During a sampling period of 100 ms, the change in mean current is much smaller than the gating-induced fluctuations; therefore the current can be considered to be essentially stationary during a period of this length, and the mean and variance measured during a succession of 100-ms epochs can be related to one another using Eq. 3.

As the Cl^- channels become activated, they produce increasing amounts of current noise. In the experiment shown in Fig. 7 *A*, current was recorded from a Jurkat T cell exposed to 67% Ringer. The fluctuations increase in amplitude as the mean current grows, reaching a peak beyond which they diminish with increasing mean current. The time course of mean current and variance from this experiment are illustrated in Fig. 7 *B*. By fitting the parabolic relation given by Eq. 3 to a plot of mean current against variance (Fig. 7 *C*), the single-channel current, i, can be estimated to be -0.12 pA at the holding potential of -60 mV. Based on the measured whole-cell reversal potential of 0 mV in this experiment, this value for i corresponds to a unitary chord conductance of 2 pS. A similar value of γ (2.4 ± 0.8 pS, $n = 3$) was obtained from measurements in murine splenic T cells (Fig. 7 *D*).

The results of the mean-variance analysis have two important implications. First, the unitary current value of -0.21 pA in Fig. 7 *D* is equivalent to a transport rate of 1.3×10^6 ions/s, ~40-fold greater than the rate of the fastest known ion carriers, valinomycin and trinactin (Hille, 1992). Thus, this result suggests that the osmotically regulated Cl^- transporter is a channel rather than a carrier, a conclusion that is also consistent with the characteristics of the current noise spectrum presented below. The second implication is that the osmotically regulated mini Cl^- channel is the most abundant of the lymphocyte channels that have been described thus far. Based on the estimate of N, the two cells in Fig. 7 each express an estimated total of ~10,000 functional Cl^- channels. When normalized to the membrane area of lymphocytes (100–1,000 μm^2, based on cell capacitance), the average surface density is estimated to be 10–100 Cl^- channels/μm^2 of membrane.

Perhaps because of their high abundance, we were unable to record distinct single Cl^- channel currents in cell-attached membrane patches. To estimate the channel's gating kinetics, the power spectrum of whole-cell Cl^- current fluctuations was analyzed. The power spectra of the data were visually fitted by a single Lorentzian function of the form

$$S(f) = S(0)/[1 + (f/f_c)^2] \tag{4}$$

where $S(f)$ is the power spectral density at frequency f, and f_c is the corner frequency at which the power is half-maximal. The data shown in Fig. 8 were collected early during the induction of g_{Cl}; at this time the estimated open probability ($I/(N \cdot i)$) was

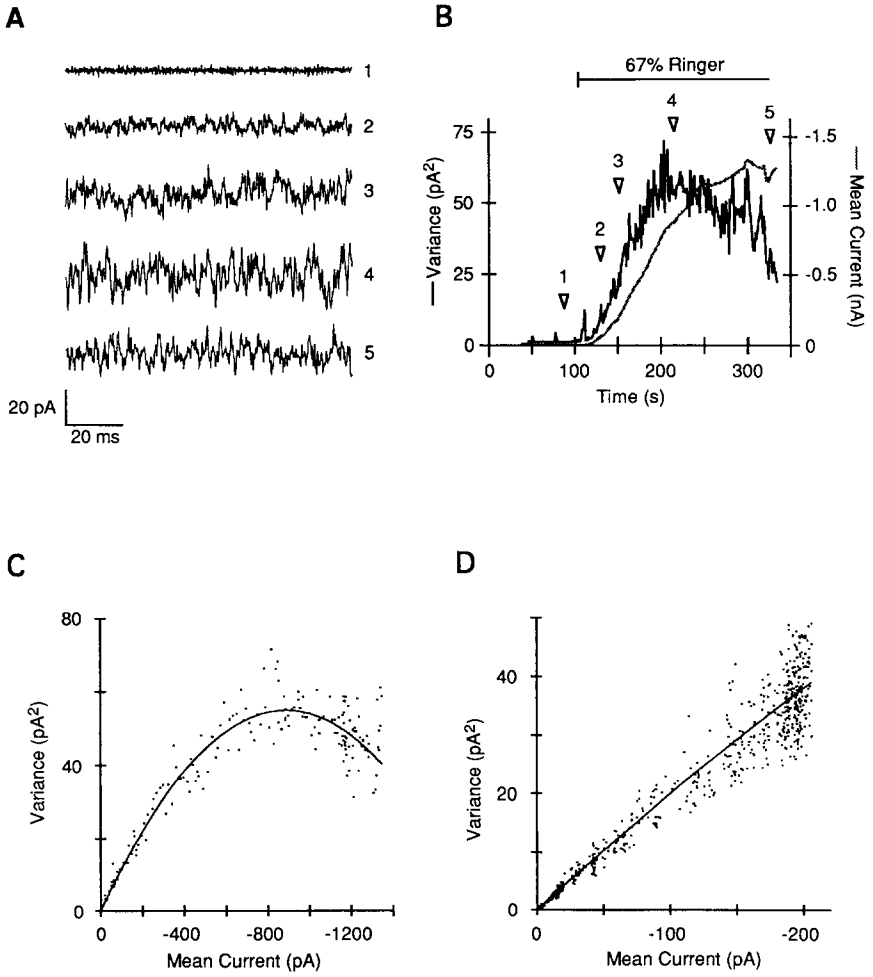

FIGURE 7. Estimation of the unitary conductance of Cl^- channels. (*A*) Single sweeps from a Jurkat T cell collected during induction of g_{Cl} at the times shown in *B*. Holding potential = −60 mV. Cell 904; KCl + ATP, isosmotic. (*B*) Mean current and variance plotted against time after break-in. Symbols numbered 1–5 mark the times at which the data in *A* were collected. (*C*) Plot of variance vs. mean current from the experiment of *A* and *B*. A parabola of the form:

$$\sigma_I^2 = iI - I^2/N$$

was fitted to the data using a nonlinear least-squares algorithm (see text), yielding estimates of N = 14,300; i = −0.12 pA; maximum open probability = 0.66. (*D*) Variance vs. mean current for a splenic T cell at a holding potential of −80 mV. The parabolic fit corresponds to estimates of N = 10,000; i = −0.21 pA; maximum open probability = 0.10. Cell 295; KCl + ATP.

~ 0.09. The fitted curve indicates a corner frequency of 386 Hz, which corresponds to a mean open time of 0.41 ms under these conditions of low open probability. These results confirm that the 2-kHz recording bandwidth of the mean-variance experiments described above was sufficiently high to allow accurate estimates of unitary

conductance. Taken together, the estimates of single-channel conductance and mean open time will provide useful constraints for later identifying the Cl^- channel in single-channel recordings.

Pharmacology

The osmotically activated Cl^- current is blocked by the stilbene disulfonates DIDS and SITS in a time- and voltage-dependent manner as shown in Fig. 9 *A*. These drugs do not appear to block at voltages between −100 and −50 mV, but blockade develops with a biexponential time course during voltage pulses to more positive potentials. Recovery after drug washout was generally incomplete, leaving a slowly decaying outward current. The biexponential development of blockade suggests that DIDS and SITS, both doubly charged anions, block the channel by binding to multiple sites within the membrane electric field. In addition, these compounds exhibit a similar value for the voltage dependence of channel blockade: an *e*-fold change of 19 ± 5 mV (n = 4) for 100 μM DIDS and 22 ± 4 mV (n = 3) for 100 μM

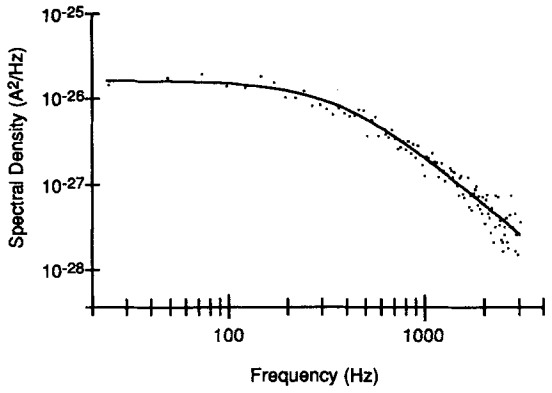

FIGURE 8. Spectral analysis of Cl^- current fluctuations in a Jurkat T cell. Data were collected during a 2.62-s period beginning at 145 s in the experiment illustrated in Fig. 7 *B*. A Lorentzian function of the form:

$$S(f) = S(0)/[1 + (f/f_c)^2]$$

was fitted by eye to the data (see text), with the following parameter values: f_c = 386 Hz, $S(0) = 1.7 \times 10^{-26}$ A^2/Hz. Cell 904; KCl + ATP, isosmotic.

SITS (data not shown). These results indicate that DIDS and SITS may bind to the same sites within the channel.

DIDS and SITS blockade increases with depolarization to a maximum level at +40 mV (see Fig. 9 *C*). At potentials above this value the block appears to decrease. One possible explanation for this result is that the block of mini Cl^- channels with DIDS and SITS is relieved at highly positive potentials. However, further experiments revealed a distinct current, independent of the swelling-induced Cl^- current, that is activated only at potentials > +40 mV and is insensitive to DIDS and SITS (data not shown). Summation of this current with the osmotically activated Cl^- current may account for the apparent relief of block above +40 mV.

The maximal degree of block is plotted against drug concentration in Fig. 9 *D*; single-site binding curves fitted to the data indicate a K_i of 17 and 89 μM for DIDS and SITS, respectively. Verapamil (100 μM) and 1,9-dideoxyforskolin (100 μM), reported blockers of the P-glycoprotein-associated Cl^- current (Valverde, Diaz,

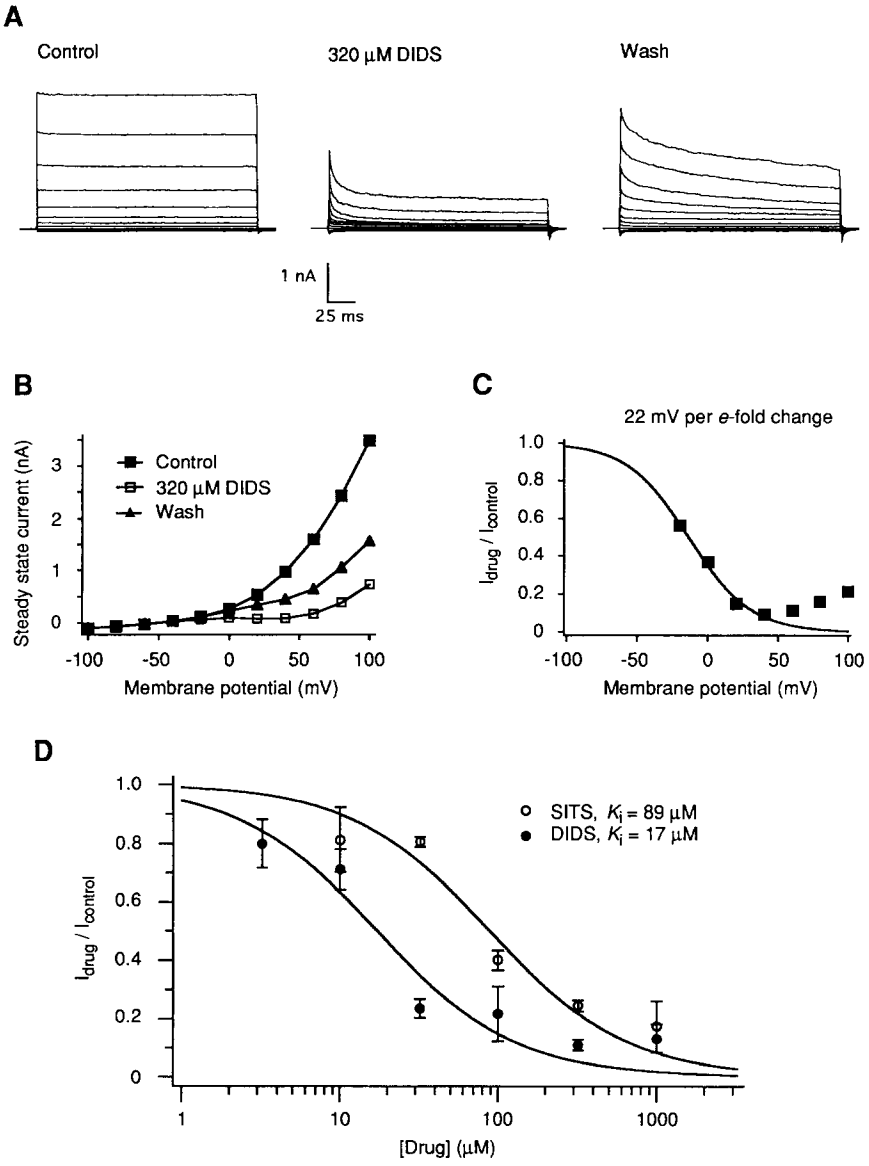

FIGURE 9. Inhibition of Cl^- current by DIDS and SITS. (*A*) Cl^- currents recorded before, during, and after application of 320 μM DIDS. Currents were evoked by 200-ms voltage steps from −100 to +100 mV in 20-mV increments from a holding potential of −60 mV. Cell 121; Cs Glu + ATP, hyperosmotic. (*B*) Steady-state current–voltage relation for the experiment shown in *A*. Current magnitudes were measured 195 ms after the start of each voltage pulse. Some distortion of the current–voltage curve can be expected at positive potentials because series resistance compensation was not used during data acquisition. (*C*) Voltage dependence of steady-state block by DIDS for the experiment shown in *A*. Block at each test potential was determined by dividing the current during drug application by the control current, both measured 195 ms after the beginning of the pulse. A Boltzmann curve of the form $I_{drug}/I_{control} = 1/(1 + \exp^{(V-V_{1/2})/k})$ was fitted to the data at potentials < +40 mV (current < 1 nA) using Igor

Sepulveda, Gill, Hyde, and Higgins, 1992), do not inhibit the osmotically activated Cl^- current (data not shown).

DISCUSSION

Mini Chloride Channels in Lymphocytes

In this paper we extend our initial characterization of an osmotically sensitive mini Cl^- channel in lymphocytes (Cahalan and Lewis, 1988). One goal of these studies is to develop a biophysical and pharmacological profile of lymphocyte Cl^- channels that will enable meaningful comparisons with Cl^- channels of other cell types and eventually the Cl^- channels encoded by cloned genes. Several features of the mini Cl^- channel readily distinguish it from the majority of known Cl^- channels. In addition to its regulation by the transmembrane osmotic gradient and membrane stretch, its most distinctive features include a small unitary conductance of 1–2 pS, an apparent lack of voltage-dependent gating, and a requirement for ATP in its activation.

Chloride currents in lymphocytes. In addition to the mini Cl^- channel described here, several other types of Cl^- channels have been reported in lymphocytes, including cAMP-, Ca^{2+}-, and volume-activated classes. Of these, the mini Cl^- channels are most similar to cAMP-activated whole-cell Cl^- current in Jurkat T cells (Maldonado, Schumann, Nghiem, Dong, and Gardner, 1991). The two currents share weak outward rectification in symmetric Cl^- solutions ($I_{Cl,+50\,mV}/I_{Cl,-50\,mV} \approx 1.4$; Fig. 6 *C*) and a lack of voltage- and time-dependent gating (Figs. 6 and 9). However, the two currents differ in that the cAMP-activated current is insensitive to block by 100 μM DIDS (cf. Fig. 9). We cannot compare the two currents at the single-channel level, as the single channels corresponding to the cAMP-activated whole-cell current have not yet been positively identified. Single-channel Cl^- currents in Jurkat cells have been described that are activated by cAMP and Ca^{2+} through the action of protein kinases (Chen, Schulman, and Gardner, 1989; Nishimoto, Wagner, Schulman, and Gardner, 1991) or by patch excision and depolarization (Garber, 1992). While these channels are similar to cAMP-activated Cl^- channels in epithelial cells that were originally proposed to underlie the Cl^- secretion defect in cystic fibrosis (Frizzell, Rechkemmer, and Shoemaker, 1986; Welsh and Liedtke, 1986), they differ significantly from the mini Cl^- channel, exhibiting stronger outward rectification ($I_{Cl,+50\,mV}/I_{Cl,-50\,mV} \approx 2.5$) and a considerably larger single-channel conductance of 40 pS measured at 0 mV. Even when adjusted for rectification of the current–voltage relation, the mini Cl^- channel has a slope conductance of only ~3 pS at 0 mV.

A Cl^- current elicited by hypotonic exposure has been observed in an EBV-

---

(WaveMetrics, Lake Oswego, OR), a Macintosh-based analysis program, indicating an *e*-fold change in blockade per 22 mV (k) and $V_{1/2} = -14$ mV. (*D*) Dose–response relations for blockade by SITS and DIDS. At least three separate experiments are represented at each drug concentration with the error bars indicating the standard deviation for each cluster. Data for each blocker, measured at +40 mV, are fit by a single binding site isotherm with a K_i of 17 μM (DIDS) or 89 μM (SITS).

transformed B cell line (McDonald, Nghiem, Gardner, and Martens, 1992). However, this current displays pronounced voltage- and time-dependent inactivation at large positive potentials, much like volume-activated Cl^- current in epithelial cells (McCann et al., 1989; Worrell et al., 1989), but unlike the osmotically activated Cl^- current we have observed in lymphocytes (see Figs. 6 and 9). In experiments using the same EBV-transformed B cell line, we have been unable to detect the inactivating Cl^- current, although the noninactivating Cl^- current becomes activated by hyposmotic challenge in the same manner as in T cells. The reason for this discrepancy is unclear at present.

Finally, T lymphocytes express maxi Cl^- channels that are easily identified on the basis of their unitary conductance of 300–400 pS and voltage- and time-dependent gating (Cahalan and Lewis, 1988; Pahapill and Schlichter, 1992). In excised patches, the maxi Cl^- channels open maximally around 0 mV, while in cell-attached patches they open with increasing hyperpolarization (Pahapill and Schlichter, 1992). Although their anion permeability sequences are similar, the mini and maxi Cl^- channels are obviously quite different in their unitary conductance and voltage dependence of gating.

Chloride currents in other cells. The lymphocyte mini Cl^- current bears a close resemblance to a chloride current that has been described recently in chromaffin cells (Doroshenko, Penner, and Neher, 1991). Similarities include (*a*) a unitary conductance of 1–2 pS estimated from noise analysis, (*b*) a lack of voltage-dependent gating, (*c*) a permeability to aspartate ~10% that of Cl^-, (*d*) weak outward rectification with symmetric Cl^- solutions, and (*e*) blockade by micromolar levels of DIDS in an apparently voltage-dependent fashion. In chromaffin cells, I_{Cl} is activated by intracellular GTPγS (Doroshenko et al., 1991) or by a positive transmembrane osmotic gradient (Doroshenko and Neher, 1992). The ATP dependence of the chromaffin cell's Cl^- current has not been investigated; however, with ATP-free internal solutions, I_{Cl} induced by a sustained osmotic gradient was transient (Doroshenko and Neher, 1992). Similar transient behavior has been noted for the osmotically activated Cl^- current in lymphocytes when ATP is omitted from the pipette solution (Ross et al., 1992). In contrast to our findings in lymphocytes (Fig. 3), pipette suction of up to −55 cm H_2O (−5.4 kPa) did not inhibit g_{Cl} induced in chromaffin cells by a moderate osmotic gradient (Doroshenko and Neher, 1992). The irreversibility of g_{Cl} in chromaffin cells may be related to the observation that a brief pulse of pipette pressure is sufficient to elicit the same sequence of Cl^- conductance changes as a sustained pressure stimulus. Thus, the proximal stimulus for Cl^- channel activation in chromaffin cells may be less direct than that in T cells, such that terminating the swelling does not immediately reduce channel activation. Pharmacological experiments have raised the possibility that Cl^- current induction in chromaffin cells may be mediated through a second messenger generated by arachidonic acid metabolism (Doroshenko, 1991; Doroshenko and Neher, 1992). We have not yet tested this possibility in T cells.

Another closely related mini Cl^- channel has been studied in mast cells (Penner, Matthews, and Neher, 1988; Matthews et al., 1989). Like the lymphocyte channel, mini Cl^- channels in mast cells have a conductance of 1–2 pS and are blocked in a partially reversible manner by micromolar levels of DIDS (Matthews et al., 1989). However, the mast cell Cl^- conductance does not appear to be modulated by cell

swelling, but is instead activated by intracellular GTPγS, cAMP, and possibly other as yet unidentified internal messengers (Matthews et al., 1989). Although regulation of the mini Cl^- channels in chromaffin cells and mast cells is different from that in lymphocytes, the similarities in channel properties suggest that they may be representatives of a class of low-conductance, voltage-independent Cl^- channels under the control of cell type–specific factors possibly related to their cell-specific functions.

Several characteristics clearly distinguish volume-regulated Cl^- channels of epithelial cells from mini Cl^- channels in lymphocytes. First, swelling-induced Cl^- conductance in cells from human airway or sweat gland epithelia and the T_{84} human colonic cell line is voltage dependent, decreasing with depolarization above −80 mV (McCann et al., 1989) and displays pronounced time-dependent inactivation during voltage steps to +60 mV or above (McCann et al., 1989; Worrell et al., 1989; Solc and Wine, 1991; Chan et al., 1992). In contrast, the lymphocyte Cl^- channels do not inactivate, even at potentials as positive as +100 mV (Fig. 9). Second, the conductance of the epithelial channels is 20–75 pS, as compared with 1–2 pS for the lymphocyte channel. A low-conductance (4.5 pS) Cl^- channel has been described in human nasal airway epithelial cells and shares a lack of inactivation with mini Cl^- channels in lymphocytes (Duszyk, French, and Man, 1992). However, these airway Cl^- channels show weaker outward rectification in symmetrical Cl^- solutions than the lymphocyte channels; and it is not known whether they are activated by cellular swelling.

A swelling-activated Cl^- conductance similar to that of epithelial cells has been linked to the P-glycoprotein gene, MDR1, in transfected 3T3 fibroblasts (Valverde et al., 1992). Like the lymphocyte channel, this current is also dependent on ATP, which is consistent with the presence of two ATP binding sites on the P-glycoprotein molecule. However, as in epithelial cells, the MDR1-associated I_{Cl} exhibits time-dependent inactivation at positive potentials. In addition, the P-glycoprotein-associated Cl^- current is inhibited by 100 μM 1,9-dideoxyforskolin (90% block) or verapamil (75% block) (Valverde et al., 1992). Neither compound at 100 μM concentration has any effect on volume-activated Cl^- current in T cells (data not shown).

Swelling-activated Cl^- channels of canine ventricular myocytes also exhibit outward rectification and voltage-independent gating, as do mini Cl^- channels in lymphocytes. In cardiac cells, Cl^- channels may play a role in adjusting the background membrane conductance after myocardial ischemia and reperfusion (Tseng, 1992), suggesting the possibility that swelling-activated Cl^- channels may carry out a variety of functional roles.

Mechanism of Chloride Channel Activation

Exposure of T cells to hyposmotic media activates mini Cl^- channels, presumably as a result of cell swelling caused by the osmotically driven influx of H_2O. However, even when the difference in osmolarity between pipette and bath solutions was relatively minor (~6%), cells appeared to swell and substantial Cl^- current was induced spontaneously (see Fig. 1). Under these conditions, restricted diffusion of large cellular ions may make the cytoplasm hyperosmotic with respect to both the pipette and bath solutions, leading to water entry from the pipette and across the cell membrane. This hypothesis was originally proposed by Worrell et al. (1989) to

explain the spontaneous induction of an osmotically sensitive Cl^- current in epithelial cells using isosmotic pipette and bath solutions. Of course, if the Cl^- channels are gated by membrane stretch, then the effect of water entry may be modulated or even superseded by effects of internal dialysis on cytoskeletal structures involved in communicating tension to the channel.

The transmembrane osmotic gradient, rather than intracellular or extracellular osmolarity alone, controls activation of the Cl^- conductance. The simplest explanation for the effects of pipette suction on g_{Cl} and observations of cell swelling during induction of g_{Cl} is that the channels are regulated by membrane stretch produced by water influx and consequent cell distension. This mode of activation is consistent with the rapid reversibility of volume-induced g_{Cl} either by pipette suction or by hyperosmotic extracellular solutions, which distinguishes the lymphocyte Cl^- conductance from that of chromaffin cells (see above). However, in light of this hypothesis it is surprising that pipette suction of only -25 to -50 cm H_2O (equivalent to an osmotic gradient of 1–2 mosM) can reverse g_{Cl} induction in the presence of an imposed transmembrane osmotic gradient of ~ 100 mosM. One possible explanation for this discrepancy is that, due to the water efflux pathway afforded by the recording pipette, H_2O entering the cell from the bath is shunted into the pipette, so that a pressure difference of only 1–2 mosM develops in the presence of an imposed 100 mosM gradient. However, this explanation is inconsistent with the observation that activation of Cl^- flux in intact T cells requires a $\geq 15\%$ decrease in extracellular osmolarity, or a decrease of ~ 30 mosM (Sarkadi et al., 1984*b*). It is possible that internal dialysis of the cell affects the cytoskeletal structure in such a way as to alter the mechanosensitivity of Cl^- channels, possibly making pipette suction more effective than expected. For example, the sensitivity of stretch-activated cation channels in muscle tissue is enhanced by cytochalasins, compounds that inhibit actin polymerization and thereby disrupt the cytoskeleton (Guharay and Sachs, 1984). Further studies on the osmotic sensitivity of mini Cl^- channels under more physiological conditions, for example, using the perforated-patch method, will be required to resolve this issue.

Other factors, in addition to membrane stretch, may be involved in Cl^- channel activation in lymphocytes. We have shown that intracellular ATP is required to support the function of Cl^- channels during whole-cell recordings. ATP may be required for phosphorylation or allosteric activation, or as an energy source for ion pumping or reorganization of cytoskeletal filaments. Further experiments with analogues of ATP will address these possibilities. Although we have not investigated the Ca^{2+} dependence of mini Cl^- channels in detail, it seems unlikely that their activation is dependent on intracellular Ca^{2+}. Normal activation was observed in whole-cell recordings conducted with internal solutions containing 10 mM EGTA and $< 10^{-8}$ M free Ca^{2+}. It is nevertheless possible that Ca^{2+} may modulate the induction of g_{Cl} by osmotic stimuli in intact cells, given that hypotonic shock evokes brief Ca^{2+} transients in intact Jurkat T cells and murine thymocytes (Ross, 1991).

A Physiological Role for Mini Cl^- Channels in Triggering the RVD Response

Accumulated evidence from a variety of cells implicates Cl^- channels and K^+ channels in the RVD response. The specific types of channels that are involved

appear to vary among cell types, but the theme common to these mechanisms involves stretch-activated channels interacting with voltage- or Ca^{2+}-gated channels. Exposure to hyposmotic media forces water entry, causing the cell to swell passively. The swelling, presumably through membrane stretch, activates the trigger channel, which has been postulated in lymphocytes to be a volume-regulated chloride channel (Grinstein et al., 1982; Grinstein, Clarke, Rothstein, and Gelfand, 1983; Cahalan and Lewis, 1988). Because the chloride equilibrium potential in lymphocytes is about −30 to −40 mV (Grinstein et al., 1982), the opening of Cl^- trigger channels would be expected to depolarize the cell and activate voltage-gated K^+ channels (Deutsch, Krause, and Lee, 1986; Cahalan and Lewis, 1988; Lee, Price, Prystowsky, and Deutsch, 1988). The combined efflux of K^+ and Cl^- would drive the membrane potential to a value between E_K and E_{Cl}, causing sustained ion transport and water efflux until the osmotic pressure declines below the threshold for activating Cl^- channels, enabling them to close. The mini Cl^- channels we describe here have several defining characteristics that match those of the Cl^- pathway in RVD studied with radioactive ion flux and fluorescent dye measurements of membrane potential. Like the mini Cl^- channel, the RVD Cl^- conductance is electrogenic but not voltage dependent, is activated within seconds by osmotic swelling, and has a selectivity sequence $SCN^- = I^- > NO_3^- > Br^- \geq Cl^-$ > acetate > gluconate (Grinstein et al., 1982). In addition, RVD is inhibited by DIDS (Lee et al., 1988; Hoffmann and Simonsen, 1989). Although higher concentrations (100–300 μM) of DIDS were required to block RVD than to block the swelling-activated Cl^- current (K_i = 17 μM), this might be expected from the voltage dependence of DIDS block given a T cell resting potential of approximately −50 mV. Finally, the rapid inhibition of RVD Cl^- conductance by cell shrinkage (Sarkadi et al., 1984*b*) is consistent with the rapid reversal of g_{Cl} activation by pipette suction or hyperosmotic external solutions (Figs. 3 and 4).

Could other known Cl^- channels in lymphocytes contribute to RVD? Some of the properties of maxi Cl^- channels recently described by Pahapill and Schlichter (1992) raise the possibility of such a role. First, maxi Cl^- channels are active in cell-attached patch recordings from resting human T cells at 37°C. Given their large unitary conductance (300–400 pS), opening of one to several Cl^- channels would be sufficient to account for the magnitude of Cl^- flux during RVD (Cahalan and Lewis, 1988), and such a mechanism would explain the sharp threshold for g_{Cl} activation by osmotic swelling (Sarkadi et al., 1984*b*). Furthermore, their open probability declines with depolarization, which might explain the slow inactivation of swelling-activated Cl^- conductance in intact T cells measured with ion fluxes (Sarkadi et al., 1984*b*). However, there is no evidence at present that maxi Cl^- channels in lymphocytes are regulated by osmotic stress. Likewise, Ca^{2+}- and cAMP-activated Cl^- currents in T cells do not appear to respond to osmotic gradients (McDonald et al., 1992).

It appears unlikely that lymphocytes would often encounter osmotic imbalances in vivo of the magnitude used here to activate Cl^- current in vitro. Alternative functions of the Cl^- channels may include control of intracellular osmotic pressure during cell growth. Incorporation of amino acids into large charged proteins may upset the Donnan equilibrium across the membrane, making the cytoplasm hyperosmotic and causing water influx. Activation of the RVD mechanism may serve to maintain

homeostasis under these conditions. Given the hypothesis that the Cl^- channels are activated by membrane stretch, they may also play a role in signal transduction, causing changes in membrane potential in response to mechanical stresses on the membrane such as might occur during lymphocyte migration through tissues and during translocation across capillary walls.

The authors gratefully acknowledge Ms. Ruth Davis and Dr. Lu Forrest for maintaining cell lines and isolating murine T cells.

This study was supported by grants NS-14609 and GM-41514 to M. D. Cahalan.

Original version received 28 October 1992 and accepted version received 16 February 1993.

REFERENCES

Cahalan, M. D., and R. S. Lewis. 1988. Role of potassium and chloride channels in volume regulation by T lymphocytes. *In* Cell Physiology of Blood. R. B. Gunn and J. C. Parker, editors. Rockefeller University Press, New York. 281–301.

Chan, H.-C., J. Goldstein, and D. J. Nelson. 1992. Alternate pathways for chloride conductance activation in normal and cystic fibrosis airway epithelial cells. *American Journal of Physiology.* 262:C1273–C1283.

Chen, J. H., H. Schulman, and P. Gardner. 1989. A cAMP-regulated chloride channel in lymphocytes that is affected in cystic fibrosis. *Science.* 243:657–660.

DeCoursey, T. E., K. G. Chandy, S. Gupta, and M. D. Cahalan. 1987. Mitogen induction of ion channels in murine T lymphocytes. *Journal of General Physiology.* 89:405–420.

Deutsch, C., D. Krause, and S. C. Lee. 1986. Voltage-gated potassium conductance in human T lymphocytes stimulated with phorbol ester. *Journal of Physiology.* 372:405–423.

Deutsch, C., and S. C. Lee. 1988. Cell volume regulation in lymphocytes. *Renal Physiology and Biochemistry.* 3–5:260–276.

Doroshenko, P. 1991. Second messengers mediating activation of chloride current by intracellular GTPγS in bovine chromaffin cells. *Journal of Physiology.* 436:725–738.

Doroshenko, P., and E. Neher. 1992. Volume-sensitive chloride conductance in bovine chromaffin cell membrane. *Journal of Physiology.* 449:197–218.

Doroshenko, P., R. Penner, and E. Neher. 1991. Novel chloride conductance in the membrane of bovine chromaffin cells activated by intracellular GTPγS. *Journal of Physiology.* 436:711–724.

Duszyk, M., A. S. French, and S. F. P. Man. 1992. Noise analysis and single-channel observations of 4 pS chloride channels in human airway epithelia. *Biophysical Journal.* 61:583–587.

Frizzell, R. A., G. Rechkemmer, and R. L. Shoemaker. 1986. Altered regulation of airway epithelial cell chloride channels in cystic fibrosis. *Science.* 233:558–560.

Garber, S. S. 1992. Outwardly rectifying chloride channels in lymphocytes. *Journal of Membrane Biology.* 127:49–56.

Grinstein, S., C. A. Clarke, A. Dupre, and A. Rothstein. 1982. Volume-induced increase of anion permeability in human lymphocytes. *Journal of General Physiology.* 80:801–823.

Grinstein, S., C. A. Clarke, A. Rothstein, and E. W. Gelfand. 1983. Volume-induced anion conductance in human B lymphocytes is cation independent. *American Journal of Physiology.* 245:C160–C163.

Grinstein, S., and S. J. Dixon. 1989. Ion transport, membrane potential, and cytoplasmic pH in lymphocytes: changes during activation. *Physiological Reviews.* 69:417–481.

Grinstein, S., and J. D. Smith. 1990. Calcium-independent cell volume regulation in human lymphocytes. *Journal of General Physiology.* 95:97–120.

Grissmer, S., R. S. Lewis, and M. D. Cahalan. 1992. Ca^{2+}-activated K^+ channels in human leukemic T cells. *Journal of General Physiology.* 99:63–84.

Guharay, F., and F. Sachs. 1984. Stretch-activated single ion channel currents in tissue-cultured embryonic chick skeletal muscle. *Journal of Physiology.* 352:685–701.

Hamill, O. P., A. Marty, E. Neher, B. Sakmann, and F. J. Sigworth. 1981. Improved patch-clamp techniques for high resolution current recording from cells and cell-free membrane patches. *Pflügers Archiv.* 391:85–100.

Hille, B. 1992. Ionic Channels of Excitable Membranes. 2nd ed. Sinauer Associates, Inc., Sunderland, MA. 312.

Hoffmann, E. K., and L. O. Simonsen. 1989. Membrane mechanisms in volume and pH regulation in vertebrate cells. *Physiological Reviews.* 69:315–382.

Horn, R., and A. Marty. 1988. Muscarinic activation of ionic currents measured by a new whole-cell recording method. *Journal of General Physiology.* 92:145–159.

Lee, S. C., M. Price, M. B. Prystowsky, and C. Deutsch. 1988. Volume response of quiescent and interleukin 2-stimulated T-lymphocytes to hypotonicity. *American Journal of Physiology.* 254:C286–C296.

Lewis, R. S., and M. D. Cahalan. 1988. Subset-specific expression of potassium channels in developing murine T lymphocytes. *Science.* 239:771–775.

Lewis, R. S., and M. D. Cahalan. 1989. Mitogen-induced oscillations of cytosolic Ca^{2+} and transmembrane Ca^{2+} current in human leukemic T cells. *Cell Regulation.* 1:99–112.

Lewis, R. S., and M. D. Cahalan. 1990. Ion channels and signal transduction in lymphocytes. *Annual Review of Physiology.* 52:413–428.

Maldonado, D., M. Schumann, P. Nghiem, Y. Dong, and P. Gardner. 1991. Prostaglandin E_1 activates a chloride current in Jurkat T lymphocytes via cAMP-dependent protein kinase. *FASEB Journal.* 5:2965–2970.

Matthews, G., E. Neher, and R. Penner. 1989. Chloride conductance activated by external agonists and internal messengers in rat peritoneal mast cells. *Journal of Physiology.* 418:131–144.

McCann, J. D., M. Li, and M. J. Welsh. 1989. Identification and regulation of whole-cell chloride currents in airway epithelium. *Journal of General Physiology.* 94:1015–1036.

McDonald, T. V., P. T. Nghiem, P. Gardner, and C. L. Martens. 1992. Human lymphocytes transcribe the cystic fibrosis transmembrane conductance regulator gene and exhibit CF-defective cAMP-regulated chloride current. *Journal of Biological Chemistry.* 267:3242–3248.

Nishimoto, I., J. A. Wagner, H. Schulman, and P. Gardner. 1991. Regulation of Cl^- channels by multifunctional CaM kinase. *Neuron.* 6:547–555.

Pahapill, P. A., and L. C. Schlichter. 1992. Cl^- channels in intact human T lymphocytes. *Journal of Membrane Biology.* 125:171–183.

Penner, R., G. Matthews, and E. Neher. 1988. Regulation of calcium influx by second messengers in rat mast cells. *Nature.* 334:499–504.

Rink, T. J., A. Sanchez, S. Grinstein, and A. Rothstein. 1983. Volume restoration in osmotically swollen lymphocytes does not involve changes in free Ca^{2+} concentration. *Biochimica et Biophysica Acta.* 762:593–596.

Ross, P. E. 1991. Hypoosmotic stress generates calcium transients in mouse thymocytes. *Biophysical Journal.* 59:598*a*. (Abstr.)

Ross, P. E., S. S. Garber, and M. D. Cahalan. 1992. Swelling induces a chloride conductance and a capacitance change in Jurkat T lymphocytes. *Biophysical Journal.* 61:A514. (Abstr.)

Sands, S. B., R. S. Lewis, and M. D. Cahalan. 1989. Charybdotoxin blocks voltage-gated K^+ channels in human and murine T lymphocytes. *Journal of General Physiology.* 93:1061–1074.

Sarkadi, B., E. Mack, and A. Rothstein. 1984*a*. Ionic events during the volume response of human

peripheral blood lymphocytes to hypotonic media. I. Distinctions between volume-activated Cl^- and K^+ conductance pathways. *Journal of General Physiology.* 83:497–512.

Sarkadi, B., E. Mack, and A. Rothstein. 1984*b*. Ionic events during the volume response of human peripheral blood lymphocytes to hypotonic media. II. Volume- and time-dependent activation and inactivation of ion transport pathways. *Journal of General Physiology.* 83:513–527.

Sigworth, F. J. 1980. The variance of sodium current fluctuations at the node of Ranvier. *Journal of Physiology.* 307:97–129.

Solc, C. K., and J. J. Wine. 1991. Swelling-induced and depolarization-induced Cl^- channels in normal and cystic fibrosis epithelial cells. *American Journal of Physiology.* 261:C658–C674.

Tseng, G.-N. 1992. Cell swelling increases membrane conductance of canine cardiac cells: evidence for a volume-sensitive Cl channel. *American Journal of Physiology.* 262:C1056–C1068.

Valverde, M. A., M. Diaz, F. V. Sepulveda, D. R. Gill, S. C. Hyde, and C. F. Higgins. 1992. Volume-regulated chloride channels associated with the human multidrug-resistance P-glycoprotein. *Nature.* 355:830–833.

Welsh, M. J., and C. M. Liedtke. 1986. Chloride and potassium channels in cystic fibrosis airway epithelia. *Nature.* 322:467–470.

Worrell, R. T., A. G. Butt, W. H. Cliff, and R. A. Frizzell. 1989. A volume-sensitive chloride conductance in human colonic cell line T84. *American Journal of Physiology.* 256:C1111–C1119.

Yamamoto, D., and N. Suzuki. 1987. Blockage of chloride channels by HEPES buffer. *Proceedings of the Royal Society of London, Series B.* 230:93–100.